Feature Matching for Aligning Historical and Modern Images

Article *in* International Journal of Computers and Their Applications · September 2014

Heider Ali
Carleton University

A.D. Whitehead
Carleton University

Feature Matching for Aligning Historical and Modern Images

Heider K. Ali*
Carleton University, Ottawa, ON, K1S 5B8, CANADA

Anthony Whitehead†
Carleton University, Ottawa, ON, K1S 5B6, CANADA

Abstract

Provision of historical information based on geographical location represents a new scope of connecting the present of a certain location or landmark with its history through a timescape panorama. This may be achieved by exploring a linear timeline of photos for certain areas and landmarks that have both historic and modern photos. Matching modern to historical images requires a special effort in the sense of dealing with historical photos which were captured by photographers of different skills using cameras from a wide range of photographic technology eras. While there are many effective matching techniques which are vector- or binary-based that perform effectively on modern digital images, they are not accurate on historic photos. Photos of different landmarks were gathered on a wide ranging timeline taken in different conditions of illumination, position, and weather. This work examines the problem of matching historical photos with modern photos of the same landmarks with the intent of hopefully registering the images to build a timescape panorama. Images were matched using standard vector-based matching techniques and binary-based techniques. Match results of these sets of images were recorded and analysed. Generally, these results show successful matching of the modern digital images, while matching historic photos to modern ones shows poor matching results. A novel application of a hybrid ORB/SURF matching technique was applied in matching modern to historic images and showed more accurate results and performs more effectively.

Key Words: Timescape, panorama, modern to historic photo matching, feature matching, photographic technique, panorama software, disparity gradient filter.

1 Introduction

Experiencing history as a dynamic experience may be possible through the exploitation of timescapes: the merging of history and geographical location in a unified scope [32]. This is achieved by sequencing (hopefully registered and properly aligned) available photos from the past up to modern times. Capturing a photo of a view of an existing historic landmark by a photographer in the past traditionally made use of photographic film. This photo typically had limited quality as it was usually only shared with a small number of friends or family of the photographer. With the invention of digital photography, the exponential growth of the World Wide Web, and the growth of photo-sharing websites such as Flickr, a massive change in the photography process and photo collections sizes has occurred. Consequently, we now have a great, ever-growing, amount of photos of places, cities, and landmarks around the world. So, matching a huge set of images of certain landmarks captured an innumerable number of times, from different viewpoints, by different photographers, with different cameras and in different weather conditions presents a challenge of dealing with such images and extracting and matching their features. These features are important for image registration and alignment and the accuracy of the matching process is crucial to the success of image registration technique [16].

Feature matching has an extensive body of research and has many applications in computer vision, image processing, pattern recognition, and object detection. One such application is the matching of modern to historic photos. Many historians, travelers, and researchers are interested in matching a set of images that represent a timeline view of certain landmarks or locations [32].

This paper examines the problems that make matching historical images to modern images a more difficult problem than one might initially assume and present an initial step towards solving the problem. Section 2 presents a look at photographic technology to better define why the problem is more difficult than modern image feature matching. Section 3 shows that existing solutions for generating panoramas fail on a dataset that has both modern and historical images. Section 4 examines the many feature extraction techniques that are typically used in feature matching of images. Some of these techniques are vector-based techniques while others; which are more recent, are binary-based techniques. Both types of techniques are applied in this work in matching modern to historic images. Section 5 reviews our findings and discusses how this problem may be solved using other techniques, such as machine learning, shape matching or other content based image retrieval techniques.

In this paper these techniques will be referred as SIFT/SIFT, in which SIFT feature detector and SIFT feature descriptor are

* Systems and Computer Engineering Department. E-mail: heider@sce.carleton.ca.
† School of Information Technology. E-mail: Anthony.Whitehead@carleton.ca

used, and SURF/SURF for SURF feature detector/descriptor combination. A novel application using the hybrid ORB detector/SURF descriptor was evaluated in this context of feature matching of modern to historic photos. The matching result of the hybrid systems exhibits more accuracy than any of six standard techniques evaluated.

2 Photographic Technology Evolution

Our timeline of photos consists of images from the early 1800's up to recent time. These photos were captured by different photographers ranging from professionals, who professionally captured images using their skills and experience, to other images that may have been captured by amateurs. Both types of photographers used the available photography technology of their time. Cameras, which have undergone significant technical changes, substantially affect the quality of the captured images. The different stages of photographic technology evolution and camera development, the characteristics of each era, and the control factors that affect the photo quality will be investigated in order to evaluate the photo sets and to suggest the best criteria for dealing with poor quality images to extract their important features.

Photography and camera technology has passed through many stages of development over generations of photographic evolution including:

- Camera obscura: an optical device dating back to ancient China and ancient Greece [7] based on the pinhole phenomenon to project an image of the scene upside-down on the viewing surface. This description is based completely on the pinhole camera (Figure 1) which is a simple camera without a lens and a single small aperture, described by Ibn Al-Haytham (Alhazen) [12] who clearly reasoned the object image appearing upside-down onto the viewing surface.

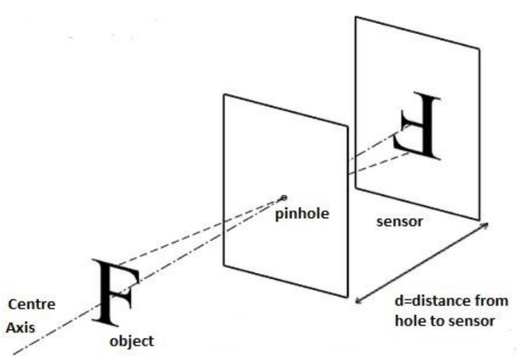

Figure 1: Geometry of a pinhole camera [20]

In a pinhole camera, the method of calculating the pinhole diameter was derived by Jozef Petzval [25]. The pinhole size is determined by the formula:

$$d = \sqrt{2 f \lambda} \quad (1)$$

Where d is the pinhole diameter, f is the focal length (distance from pinhole to image plane) and λ is the wavelength of light.

The next evolutionary step was the addition of lenses to a pinhole camera, which creates a much larger hole through which light can make it onto the film. The result of this was that more light could enter the camera and the film can be exposed faster (Figure 2).

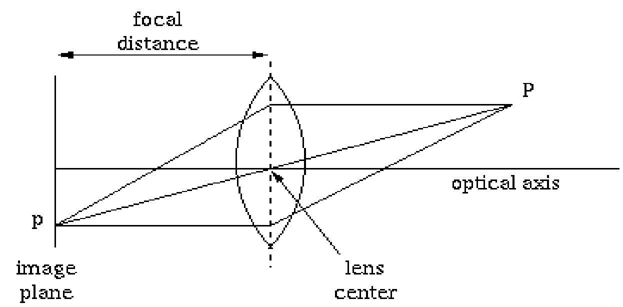

Figure 2: Pinhole with lens [29]

- Daguerreotypes cameras were introduced in 1839 and were the first publicly announced photographic process to come into widespread use [17].
- Calotypes were an early photographic process using a paper coated with silver iodide introduced by W. Fox Talbot. It needed a very long exposure (for an hour or more) to produce a negative[18].
- Dry plate, also known as gelatin process, was invented in 1871 by Dr. Richard L. Maddox. In 1879 the first dry plate factory was established [9].
- Photographic film is a sheet or strip of transparent plastic film base coated with a gelatin emulsion containing a very tiny light-sensitive silver halide crystal on one side. The characteristics of these crystals like the size determine the contrast, sensitivity and resolution of the film [11].
- Digital cameras encode images and video digitally and store them for later projection or reproduction. Digital and film cameras share an optical system by using lenses with a variable diaphragm to focus light onto an image recording device [22]. The shutter and diaphragm permit the suitable amount of light to the imaging surface similar to film but the image recording device is electronic rather than chemical (Figure 3).

The processes of capturing images from as early as 1839 to as recent as 2014 involve a variety of image capture mechanism from physical, chemical and electronic. In all cases the digitization process is affected by the capture process.

Because of the varying mechanisms for capturing an image inherent in a timeline based data set, the underlying data that makes up these images (once digitized) do not necessarily maintain the same properties. As such, it becomes difficult to match patterns in the image data using traditional techniques that imagine a homogenous capture system.

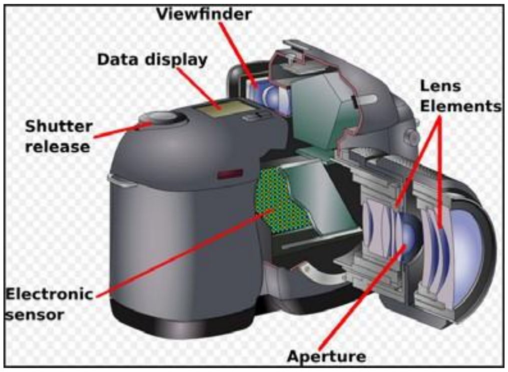

Figure 3: Digital Camera elements [8]

2.1 Technical Aspects of Photography.

Photographers control the camera by controlling many factors and adjusting the amount of light exposure to which the imaging medium is exposed, creating the latent image on the film, orvia electronics (CCD or CMOS, for example). In all cameras the process of obtaining a suitable exposure involves a few controls, manually or automatically, to insure producing a clear, sharp and well-illuminated photo [11]. The controls include but are not limited to:

- Focal length: the distance from the lens center to the image plane.
- Aperture: The adjustment of lens opening and represented by the f-number, which controls the amount of light passing through the lens and is calculated by dividing the distance from the pinhole to the imaging plane (the focal length) by the diameter of the pinhole. Aperture affects the depth of field; the higher the f-number and the smaller the opening, the greater the depth of field and hence more diffraction blur [1]. The effective aperture diameter is found by dividing the focal length by the f-number.
- Type of lens: normal, long, focus, wide angle, telephoto, macro, fisheye, or zoom [10], lenses affect the overall light hitting the imaging media.
- Focus: Adjusting the position of a viewed object relative to the camera as in focus or out focus. Focus affects the sharpness of a captured image.
- Shutter speed: The shutter controls the amount of time during which the imaging medium is exposed to light for each exposure [10]. This affects the contrast and illumination of the resulting image.
- Metering: Controlling the highlights and shadows according to the photographer desire by the exposure measurement. Artistic desire will affect the image quality.
- ISO speed: Numerical indicator of the gain from light to adjust the automatic exposure system [10].
- Inherent sensitivity of the recording medium to the light color/wavelengths and intensity [10]. This affects required exposure times and affects the imaging processes with motion blur and other speed-based artifacts.

2.2 Exposure and Rendering.

These camera control factors are interrelated and the exposure changes with:

- exposure duration
- aperture of lens, and
- the effective focal length of lens

To model these control factors mathematically, we would end up with an underdetermined system because we have multiple variables (such as those listed above) and only a single image with which to determine the exact configuration.

2.3 Historic Photos.

Our timeline dataset consists of many landmarks composed of historic and modern photos for a period of time extending from the 1800's up to modern time. Generally, the modern photos were captured by digital cameras with a sophisticated lens system and the information about the camera, such as focal length, camera parameters and lens data are most likely available in the EXIF data embedded inside the image file. On the other hand, the historic photos are significantly more challenging due to missing camera information, imprecise lenses and poor capture conditions. Some of the factors that lead to poor historic photos include:

- Historic photos captured in the pinhole camera era are, as a consequence, either uncontrollable or very few control factors are monitored by the photographers.
- The pinhole camera in its basic structure has no lens, and the aperture adjustment differs in a manner which provides a little control on the light exposure.
- Pinhole cameras have infinite depth of field. The selection of pinhole size may lead to problematic situations. The smaller pinhole is supposed to result in sharper image resolution, but an extremely small hole may produce diffraction effects and a less clear image due to the light wave property [17]. As well, vignetting may occur as the diameter of the hole approaches the thickness of the material in which it is punched.
- As the lenses were added to the pinhole camera model to create softer and more controllable images, this leads to difficulties in dealing with historic photos due to missing all or some of the following control information: aperture, focal length, shutter speed, lens and exposure details.
- Noise and uncontrollable effects through the image capturing environment, such as dust on the film, or the film development process.
- Missing information of filters which may be placed between the object and the image producing recording medium.

In this section we have highlighted a number of issues in the capture processes that differ between modern and historic images and the litany of issues that are created when using historic images for matching. We next examine the state of the art solutions that are available for image matching and registration when they are applied to datasets such as ours that include modern and historic images of the same landmark.

3 Timeline-Based Image Datasets in Panoramic Software

To investigate the behavior of our data-set of modern and historic images which have been captured by different photographers, by different cameras and photographic technologies under different capture environments, we apply our data-set on a number of available panorama building softwares to analyze how these panorama applications behave. If successful, aligned images should result on the historic and modern photos as these applications attempt build a panoramic view.

We used four commercial panorama building applications with different features for dealing with missing or incomplete control factors. The panorama building applications used on our data sets are: PTGui [24], ArcSoft Panorama Maker [2], PhotoStitcher [23], and Kolor AutopanoGiga [4].

3.1 Data Set Description.

Capturing a photo of a view of an existing historic landmark by a photographer in the past traditionally made use of photographic film. A photo set of famous landmarks in the world has been gathered from Flockr.com and Google images websites. These photos captured images an innumerable number of times, from different viewpoints, by different photographers, with different cameras and weather conditions. Figure 4 shows a timeline of a set of photos for 3 landmarks ordered in ascending order. The full set of these images includes 10 landmarks and 10 images for each landmark that are used in the evaluation of modern to historic photo matching.

3.2 Panorama Software on Modern Landmark Images.

To test the behavior of these panorama making applications on modern landmark images, modern images of the Parliament of Canada were selected and applied successfully as seen by the example panoramas in Figures 5 and 6**.**

3.3 Panorama Software on Timeline of Modern and Historic Landmark Images.

We applied the timeline dataset which includes both modern and historic photos of the Canadian Parliament building landmark. The unsuccessful results are displayed in Figures 7, 8 and 9.

We then attempted to apply the entire set of datasets of our 10 landmarks on these four panorama building applications. We summarize the results in Table 1 below and present a sample of these attempts on some of these timelined datasets in Figures 10 and 11.

Figure 4: Sample images of three famous landmarks ordered in ascending order from our test data set

Figure 5: Panorama software on modern landmark images (Parliament of Canada) – ArcSoft Panorama Maker

Figure 6: Panorama Software on Modern landmark images (Parliament of Canada) – PTGui Panorama Building Software

Figure 7: Panorama software on timeline image set of Parliament of Canada landmark- PTGui panorama software

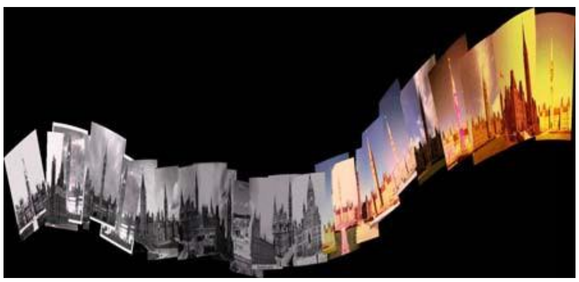

Figure 8: Panorama software on timeline image set of Parliament of Canada landmark- ArcSoft panorama maker

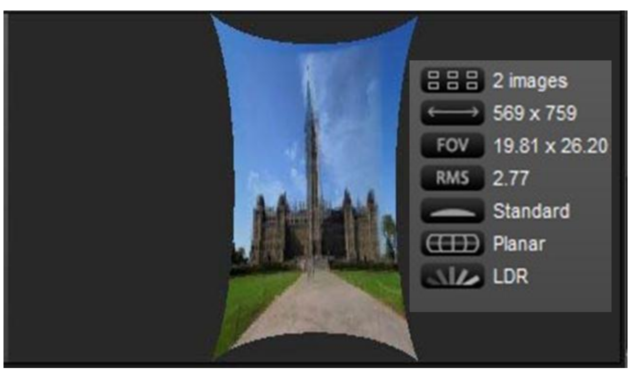

Figure 9: Panorama software on timeline image set of Parliament of Canada landmark- Autopano Giga panorama building software with the report of this attempt

In Table 1, we can note that PTGui produced a preview of 2 images out of the landmark timeline photo set and discarded other photos in which features could not be extracted (Figure 7). In other cases PTGui failed to build a panorama at all, so, it presents only the first image of the landmark timeline set (Figure 11). ArcSoft also failed to build any type of panorama; instead it tried to show a sequentially lined-up set of photos keeping their time order without any physical alignment (Figure 8). The Kolor Autopano Giga software failed, in most cases, to build a panorama and arranged them one over the other without any type of physical alignment or linking (Figure 10b). In only one case, this software made a simple panorama of only 2 images from which it extracted recognizable features (Figure 9). Finally, the Photo Stitcher software failed in all cases to build a panorama and shows the last image, except for one case, where it shows a panorama of some images of data set (Figure 10c).

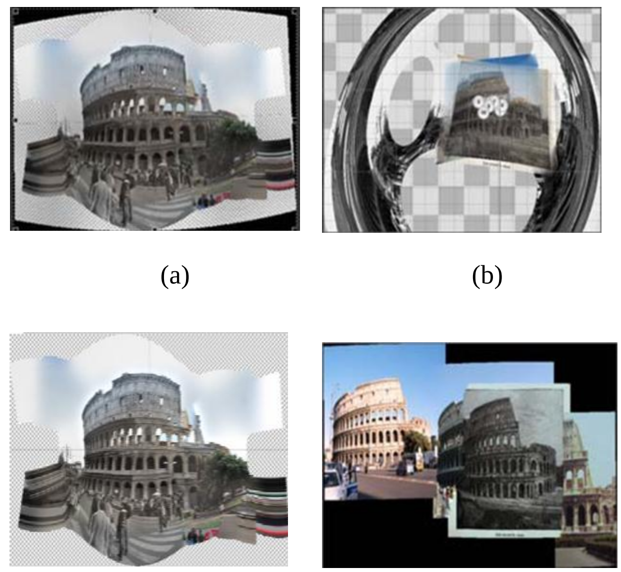

(a) (b)

(c) (d)

Figure 10 Panorama software on timeline image set of coliseum landmark (a) ArcSoft panorama maker (b) PTGui (c) PhotoStitcher (d) Kolor Autopano Giga panorama software

(a) (b) (c)

Figure 11: Application of PTGui software on many of landmarks timelined photos (a) Dome Rock (no panorama) (b) Eiffel Tower (no panorama) (c) Empire State Building (no panorama)

Table 1: Panorama building applications on many timelined photo landmarks

Landmark	Panorama Software (Produce Aligned Panorama)			
	PTGui	ArcSoft	Kolor Autopano Giga	Photo Stitcher
Parliament of Canada	Yes(Produced Preview of 2 Images)	No(Sequentially Lined-up images)	Yes(2 out of 35 Images)	No(Shows only Last image)
Coliseum	Yes(Produced Preview of 2 Images)	No(Sequentially Lined-up images)	No(Arranged Layered images)	Yes
Dome	No	No(Sequentially Lined-up images)	No(Arranged Layered images)	No(Shows only Last image)
Eiffel	No(Shows Only First image)	No(Sequentially Lined-up images)	No(Layered)	No(Shows only Last image)
Hagia-Sofia	No(Shows Only First image)	No(Sequentially Lined-up images)	No(Arranged Layered images)	No(Shows only Last image)
Machu	No(Shows Only First image)	No(Sequentially Lined-up images)	No(Arranged Layered images)	No(Shows only Last image)
Pyramid	No(Shows Only First image)	No(Sequentially Lined-up images)	No(Arranged Layered images)	No(Shows only Last image)

The overall results shown in Table 1 indicate that:

- All the software analyzes the images to detect the available control points in the overlapped areas of the images used in stitching to properly build a panorama
- The behavior of the panorama making software in dealing with our datasets of images which contains mixed images of modern and historic photos can be categorized three ways:

1) Build a panorama overview from a subset of images containing shared control points and discard other images (PTGui). This is the best type performance
2) Simply layering the images as they were sequentially presented without building a panorama (ArcSoft Panorama Maker).
3) Produce a single unregistered view of images as they layered one over others using a type of alpha-blending on the images (Kolor Autopano Giga)

Hence, we can conclude that:

- The available commercial panorama making software is unable to deal with historic photos.
- They achieve limited success in stitching only a subset of images (but only the modern ones).
- Completely fail at the process of matching and aligning a timeline-based dataset of images as required to build a timescape presentation.

4 Feature Matching

4.1 Related Work.

In this review of the related work, we will explore the literature around two key areas; the first is the research work in matching modern to historic photos, while the second is the feature matching techniques.

4.1.1 Modern to Historic Photo Matching. There are few attempts in matching modern to historic photos. Uttama et al [31] proposed a technique for indexing and matching the historic images with each other depending on the available database, however photo matching was not their end goal. Snavely et al [27] concentrated on finding photo paths and turning them into controls for image-based rendering but focused use with modern digital imagery. Snavely et al [28] presented algorithms for structure-from-motion and image-based rendering for the 3D scene modeling and visualization. Agarwal et al [3] showed how to find edges connecting two images if matching features were found between them depending on the match graph to get as comprehensive a reconstruction as possible. It should be noted that the range of dates in these image sets is relatively small in comparison to what is proposed here and none of the above expect to use historical images.

4.1.2 Feature Matching Techniques. There are a number of opportunities to match images that may include shape, color and texture. However, as our goal is to register images to generate views from the same point, we require a number of point features to compute the warp matrix accurately. For good alignment, we need accurate point correspondences. As such we are examining point feature matching techniques only in this work. To achieve effective matching, we generally seek invariant properties [19] so that the extraction result does not vary according to chosen (or imposed) conditions. As an essential invariant, we are looking for immunity to changes in illumination level, scale, location, rotation, or viewpoint [19]. A wide range of feature detectors and descriptors have been presented in the literature. A widely known and used detector is the Harris detector [13] which is based on the eigenvalues of the second-moment matrix, but Harris corners are not scale invariant and hence, it is not applicable in our application.

Lowe [15] proposed the well-known technique SIFT for extracting invariant features from images which implies both detector and descriptor. SIFT is invariant to scale, rotation, illumination and viewpoint changes. Ke and Sukthankar [14] introduced a local image descriptor by applying Principal Components Analysis (PCA) to the normalized gradient patch to get more distinctive, more robust image deformation, and more compact than the standard SIFT representation.

Bay et al [5] proposed the scale- and rotation –invariant interest point (SURF) detector and descriptor. The detector is based on the Hessian matrix and relies on the integral images to reduce the computation time and the descriptor describes a distribution of Haar-wavelet responses within the interest point neighborhood to introduce the descriptor of 64-D length. These feature matching techniques are vector-based, which offer efficient individual computation but they suffer from a computational complexity as numbers of features grow. On the other hand, the binary descriptors proposed an alternative to minimize the computation time and to keep the descriptors robustness and efficiency. Calonder et al [6] proposed to use binary strings as an efficient feature point descriptor and presented a BRIEF binary descriptor of 256 bits length. BRIEF suffers from high sensitivity to image rotation and scale changes. Rosten et al [25] proposed a feature detector (FAST) which is based on machine learning and depends on the segment test criterion. FAST has been improved by using machine learning to address the problem of the ordering and distribution of corner appearance. Rublee et al [26] based on the FAST keypoint detector and the BRIEF descriptor proposed a very fast binary descriptor called ORB (Oriented FAST and Rotated BRIEF) which is rotation invariant and resistant to noise. Alahi et al [1] proposed a keypoint descriptor Fast Retina Key point (FREAK) inspired by the retina of the human visual system by computing a cascade of binary strings through the comparing of image intensities over a retina sampling pattern. We next outline the modern to historic feature matching problem and evaluation performed.

4.2 Feature Detection and Matching

Six standard feature extraction techniques were selected to be applied on our test set of historic and modern images. These are Harris, BRIEF, BRISK, SIFT, SURF and ORB which are selected to evaluate against our set of photos which are taken over a long timeline and under different conditions. The matching will be performed on ten images covering the timeline for ten famous landmarks. Each image of a landmark will be matched with all other images of a landmark to get the matching results. These results have been analyzed to discover the strengths and weaknesses of each technique and hence to decide the suitability of these techniques to our application. Then, we follow up with the novel hybrid ORB/SURF technique and its results.

4.2.1 Matching Procedure. The preliminary keypoint matching on two images using any technique reveals too many matching points which include a large number of outliers. Figure 12 shows an example of two images from different times being compared using SURF as keypoint detector and descriptor. The keypoint matching was performed using BruteForce matching algorithm which matches *N* feature descriptors of the source image with *N* feature descriptors of the target image. In these *N*x*N* features, for each feature descriptor of the feature set of the source image this matcher will find the closest descriptor in the feature set of the target image by trying each descriptor in the target set [21]. The result of BruteForce matching of images (a) and (b) of Figure 12 is shown in (c). This technique produces best results with minimal number of outliers in keypoints of the two matched images.

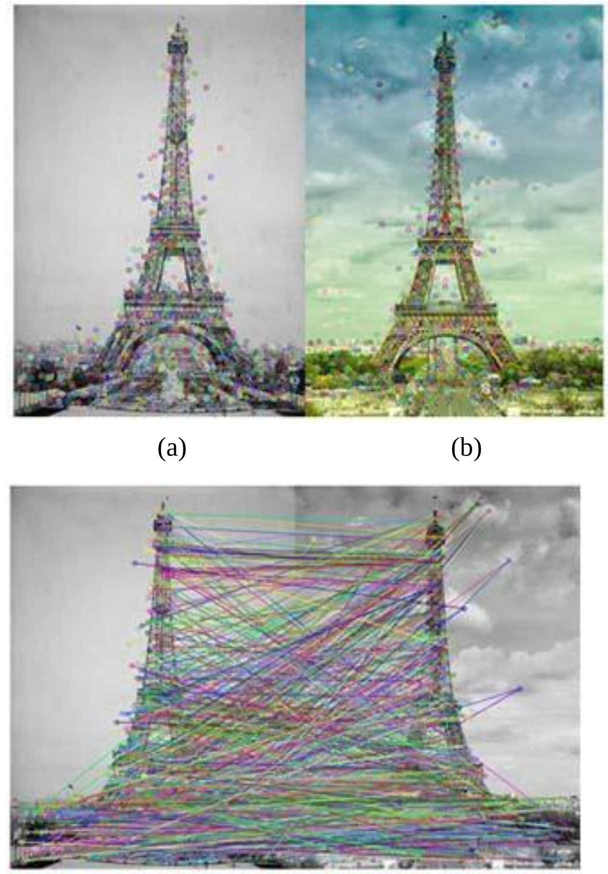

(a) (b)

(c)

Figure 12: Eiffel tower (a) Image taken in 1889 (b) Image taken in 2013 (c) SURF/SURF matching of left keypoints with those on right image using Brute Force algorithm

4.2.2 Disparity Gradient Filter. To discard outliers and achieve a better matching accuracy, the disparity gradient filter was applied. A disparity gradient filter works on motion vectors and removes outlier matches based on their deviation from the median of the whole set [30]. The disparity gradient was originally developed as a method used to reliably decide how to fuse images in stereo vision [30]:

$$d = | r_L - r_R | / \frac{1}{2} | r_L + r_R | \qquad (2)$$

Where d is the disparity gradient vector r_L in the left image and the corresponding vector r_R is in the right image.

The disparity gradient filter (DGF) applied to a pair of images on the matching keypoints is extracted using SURF/SURF, and the results are shown in Figure 13.

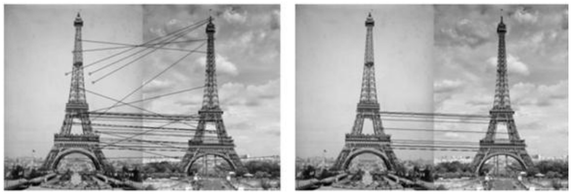

(a) (b)

Figure 13: Applying disparity gradient filter (DGF) on features extracted using SURF/SURF (a) Before applying DGF (b) After applying DGF

4.3 Feature Matching Evaluations

Our ORB/SURF approach is inspired by two techniques and based on our attempt to match modern to historic images. These two techniques represent the base of our approach because the SURF descriptor has become a *de facto* standard for fast computation descriptors and is vector-based while ORB detector takes advantage of its dependency on the intensity threshold parameter between the center pixel and the circular ring about the center with a measure of cornerness which is enhanced by a scale-pyramid of the image and binary-based detector. These two techniques were applied separately on our data set, and we integrated them into our hybrid ORB/SURF extractor and applied it on the same image set. Matching was applied on each image with all other images in the set and with itself and each landmark set contains a timeline of 10 images. So, 100 matches were done on each time-based set of images for each landmark.

The results are shown in the following three subsections.

4.3.1 SURF/SURF. The SURF detector and descriptor invariant properties to scale and rotation changes was achieved through relying on integral images to reduce the computation time by using a Hessian matrix-based measures for the detector and a distribution-based descriptor [14]. The integral images allow the fast computation of the box type convolution filters, the entry of the integral image $I_{\sum}(x)$ at a location $a=(x\ \ ,y)^T$ represents the sum of all pixels of the input image I within a rectangular region formed by the origin and a:

$$I_{\sum}(x) = \sum_{i=0}^{i\leq x} \sum_{j=0}^{j\leq y} I(i,j) \qquad (3)$$

While the Hessian matrix based interest points, for a point $a=(x\ \ ,y)$ in an image I, the Hessian matrix $H(a, \sigma)$ in a at scale σ *is* defined as follows:

$$H(a,\sigma) = \begin{bmatrix} L_{xx}(x,\sigma) & L_{xy}(x,\sigma) \\ L_{yx}(x,\sigma) & L_{yy}(x,\sigma) \end{bmatrix} \qquad (4)$$

Where $L_{xx}(x,\sigma)$ is the convolution of the Gaussian second order derivative $\frac{\partial^2}{\partial x^2} g(\sigma)$ with the image I in point a.

The descriptor describes a distribution of Haar-wavelet responses within the interest point. The Haar response in horizontal direction called d_x and the Haar wavelet response in vertical direction is called d_y which are summed over each sub-region and form a first set of entries in the feature vector. So, each sub-region has a four-dimensional descriptor vector **v** for the interested structure:

$$\mathbf{v} = \left(\sum dx, \sum |dx|, \sum dy, \sum |dy|\right) \qquad (5)$$

The successful matching is marked as 1 and displayed in green while the failed matching is marked as 0 and displayed in red. The SURF detector/ SURF descriptor was applied to the complete image set of the 10 landmarks, the matching results of these images for the Empire building shown in Table 3.

Table 3: Empire state building landmark matching using SURF/SURF matcher

SURF/SURF	1936	1940	1942	1955	1957	1959	1996	2007	2007b	2011
1936	1	1	0	0	0	0	0	1	0	1
1940	1	1	1	1	1	0	0	0	0	0
1942	0	0	1	1	0	0	1	0	0	0
1955	0	0	0	1	0	0	1	1	1	1
1957	1	0	1	1	1	1	0	1	0	0
1959	0	1	0	1	1	1	0	1	1	1
1996	0	0	0	0	0	1	1	1	1	1
2007	0	0	0	0	0	1	1	1	0	1
2007b	0	1	1	0	0	1	1	0	1	0
2011	0	0	0	0	0	0	0	1	0	1

4.3.2 ORB/ORB. In an attempt to exploit the binary-based feature of the ORB (Oriented FAST and Rotated BRIEF) technique and to test the suitability of this technique to the modern to historic image matching, we apply it to our image set. The ORB detector, which is called oFAST as FAST keypoint Orientation, is based on the FAST detector; which takes one parameter, the intensity threshold between the center pixel and those in a circular ring about the center, oFAST uses a simple measure of corner orientation, the intensity centroid [26] which assumes that a corner's intensity is offset from its center, and this vector used to refer an orientation. The moments of patch is defined as [26]:

$$m_{pq} = \sum_{x,y} x^p y^q I(x,y) \qquad (6)$$

with these moments, the centroid is found as [11]:

$$C = \left(\frac{m_{10}}{m_{00}}, \frac{m_{01}}{m_{00}}\right) \qquad (7)$$

So, the vector from the corner's center, O, to the centroid can be constructed. The Orientation of the patch is:

$$\Theta = atan\,(m01,\ m10) \qquad (8)$$

The ORB/ORB was applied to the complete image set of the 10 landmarks, the matching results of these images for the Eiffel tower shown in Table 4.

Table 4: Eiffel landmark matching using ORB/ORB matcher

ORB/ORB	1889	1889b	1890	1937	1945	1967	1967b	1986	2005	2011
1889	1	0	0	0	0	0	0	0	0	0
1889b	0	1	0	0	0	0	0	0	0	0
1890	0	0	1	0	0	0	0	0	0	0
1937	0	0	0	1	0	0	0	0	0	0
1945	0	1	0	1	1	0	0	0	0	0
1967	1	1	0	1	0	1	1	0	0	1
1967b	0	0	0	0	0	0	1	0	0	0
1986	0	0	0	0	0	0	0	1	0	0
2005	0	0	0	0	0	0	0	0	1	1
2011	0	0	0	0	0	0	0	0	0	1

4.3.3 Hybrid ORB Detector /SURF Descriptor. To get an effective image matching technique, a novel hybrid ORB/SURF is tested by using the ORB detector, which is based on the use of machine learning to address the problem of the ordering distribution of corner appearance, and the SURF descriptor which is vector-based and generated through defining a subregion around the identified feature with array elements consists of 64 floating-point numbers generated depending on the reproducible orientation of the descriptor. This hybrid ORB/SURF outperforms the performance of other used standard image matching techniques (SIFT/SIFT, SURF/SURF and ORB/ORB).

Hybrid ORB/SURF improved the feature matching of the modern to historic images of SURF/SURF by a high margin as shown in Tables 3 and 5 by comparing matching results of the Empire State Building landmark, as the blue cells in Table 5 refer to improvement in matching process compared to Table 3 results. The matching results of ORB/SURF are shown in Table 5.

Table 5: Empire State Building landmark matching using ORB/SURF matcher

ORB/SURF	1936	1940	1942	1955	1957	1959	1996	2007	2007b	2011
1936	1	1	2	0	2	0	0	1	0	1
1940	1	1	1	1	1	2	0	0	2	0
1942	0	2	1	1	0	2	1	2	2	2
1955	0	0	0	1	2	2	1	1	1	1
1957	1	0	1	1	1	1	2	1	0	2
1959	0	1	2	1	1	1	0	1	1	1
1996	0	0	0	0	0	1	1	1	1	1
2007	2	0	2	2	0	1	1	1	0	1
2007b	0	1	1	0	0	1	1	0	1	0
2011	0	2	2	2	2	2	2	1	2	1

For a comprehensive view of all applied feature extraction techniques, all the results of the application of these techniques on the Empire State Building landmark are shown in Appendix A.

4.4 Other Feature Matching Techniques Applied to Image Sets

To analyze the performance of our approach comparing different feature extraction techniques on modern to historic images, two standard techniques and two modern techniques were applied. The two main techniques (Harris corner detector and SIFT/SIFT) and the recent techniques (BRIEF/BRIEF and BRISK/BRISK) were applied on ten famous landmarks.

4.4.1 Harris Corner Detector. The widely known and used detector was the Harris detector [13], which is based on the eigenvalues of the second-moment matrix and was applied on our data set of historic and modern images of landmarks. Figure 14a shows the result of matching the results of two images of the pyramid landmark; one is historic and belongs to 1880 while the other is modern and belongs to 2006. Figure 14b shows the matching of a historic image of 1880 with itself and Table 6 shows the complete matching results of the images of the pyramid landmark.

(a)

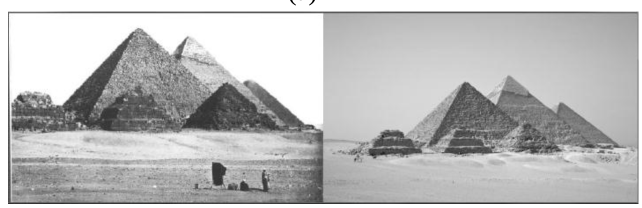

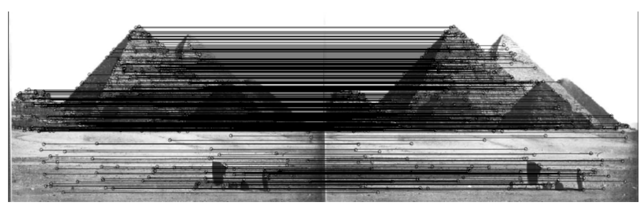

(b)

Figure 14: Applying HARRIS/HARRIS feature extraction on (a) images of 1880 with image of 2006 and (b) image of 1880 with itself for the Pyramid landmark

Table 6: Pyramid landmark matching using HARRIS/HARRIS matcher

HARRIS/HARRIS	1858	1880	1940	1969	1978	1992	1996	2006	2011	unknown
1858	1	0	0	0	0	0	0	0	0	0
1880	0	1	0	0	0	0	0	0	0	0
1940	0	0	1	0	0	0	0	0	0	0
1969	0	0	0	1	0	0	1	0	0	0
1978	0	0	0	0	1	0	0	0	0	0
1992	0	0	0	0	0	1	0	0	0	0
1996	0	0	1	0	0	0	1	0	0	0
2006	0	0	0	0	0	0	0	1	0	0
2011	0	0	0	0	0	0	0	0	1	0
unknown	0	0	0	0	0	0	0	0	0	1

4.4.2 SIFT/SIFT. Due to the invariant properties of SIFT algorithm its descriptor had been applied to the test set images. The scale invariance realized through the application of scale space principle by detecting stable keypoint locations using scale-space extrema in the difference-of-Gaussian (*DoG*) function convolved with image $D(x, y, \sigma)$, which can be computed from the difference of two nearby scales separated by a constant multiplicative factor *k*[8] :

$$D(x, y, \sigma) = (G(x, y, k\sigma) - G(x, y, \sigma)) * I(x,y) \qquad (9)$$

Where $G(x, y, \sigma) = \frac{1}{2\pi\sigma} e^{-(x2 + y2)/2\sigma 2}$

The detector is computed by assigning a consistent orientation to each keypoint based on image properties. The Gaussian smoothed image *L* with the closest scale is used in the computation of gradient magnitude, $m(x,y)$ and orientation, $\theta(x,y)$ are computed using pixel difference:

$$m(x,y) = \sqrt{(L(x+1,y) - L(x-1,y))^2 + (L(x,y+1) - L(x,y-1))^2} \qquad (10)$$

$$\theta(x,y) = \tan^{-1}((L(x,y+1) - L(x,y-1))/(L(x+1,y) - L(x-1,y))) \qquad (11)$$

Table 7: Eiffel landmark matching using SIFT/SIFT matcher

SIFT/SIFT	1889	1889b	1890	1937	1945	1967	1967b	1986	2005	2011
1889	1	0	0	1	0	1	1	1	0	0
1889b	0	1	1	1	0	1	1	0	0	0
1890	1	1	1	1	1	1	0	1	0	0
1937	1	1	1	1	1	1	1	1	1	1
1945	0	0	1	0	1	1	1	1	0	1
1967	1	1	1	1	1	1	1	1	0	1
1967b	1	1	1	1	1	1	1	1	0	1
1986	0	0	1	1	1	1	1	1	1	1
2005	0	0	1	1	0	0	1	1	1	1
2011	1	0	0	1	1	1	1	1	1	1

The matching results of one of the landmarks, which is the Eiffel Tower, are shown in Table 7 while the other SIFT/SIFT matching results of the other nine landmarks are shown in the accuracy table shown in the results section.


(a)


(b)

Figure 15: Keypoint matching of images of Eiffel Tower (a) Bad matching in the pair 1889-2005 and (b) Successful matching in the pair of 1945-1967b

It should be noted that this example is the highest accuracy within the dataset. SIFT/SIFT technique shows a bad matching on the image pair 1889-2005 in image (a) and successful matching for the pair 1945-1967 in image (b) of Figure 15. Of note, the corners representing matching efforts of the oldest (historic) to the newest (modern) images are where the failures are most common.

4.4.3 BRIEF/BRIEF. The BRIEF descriptor is based on a relatively small number of intensity different tests to represent the descriptor as a binary string and yields high recognition rates [6]. Figure 16 (a) and (b) shows the application of BRIEF/BRIEF feature extractor on the image set of the Whitehouse landmark, while Table 8 shows the full matching results of the set of this landmark using BRIEF/BRIEF.


(a)


(b)

Figure 16: Applying BRIEF/BRIEF feature extraction on (a) images of 1993 and 2012 and (b) on images pair 1948- 2009 for the Whitehouse landmark

Table 8: Whitehouse landmark matching using BRIEF/BRIEF matcher

BRIEF/BRI EF	1863	1945	1948	1965	1966	1993	2009	2009b	2012	2012b
1863	1	0	0	0	0	0	0	0	0	0
1945	0	1	0	0	0	0	0	0	0	0
1948	0	0	1	0	0	0	0	1	0	0
1965	0	0	0	1	0	0	0	0	0	0
1966	0	0	0	0	1	0	0	0	0	0
1993	0	0	0	0	0	1	0	0	1	0
2009	0	0	0	0	0	0	1	0	0	0
2009b	0	0	1	0	0	1	0	1	0	1
2012	0	0	0	0	0	0	0	0	1	0
2012b	0	0	0	0	0	1	0	1	0	1

4.4.4 BRISK/BRISK. The BRISK keypoints detector and descriptor based a sufficient prior knowledge on the scene and camera. BRISK computes brightness comparisons by configuring a circular sampling pattern from which it forms a binary descriptor string. Figure 17 shows the application of BRISK/BRISK extractor on two images of the Stonehenge landmark while Table 9 shows the complete matching results on the image set of the Stonehenge landmark.

Figure 17: Applying BRISK/BRISK feature extraction on the pair image of 1955-2009 for the Stonehenge landmark

Table 9: Stonehenge landmark matching using BRISK/BRISK matcher

BRISK/BRISK	1887	1908	1928	1955	1955b	2007	2008	2009	2011	unknown
1887	1	0	0	0	0	0	0	0	0	0
1908	0	1	0	0	0	0	0	0	0	0
1928	0	0	1	0	0	0	0	0	0	0
1955	0	0	0	1	0	0	0	0	0	0
1955b	0	0	1	0	1	0	0	0	0	0
2007	0	0	0	0	0	1	0	0	0	0
2008	0	0	0	0	0	0	1	0	0	0
2009	0	0	0	0	0	0	0	1	0	0
2011	0	0	0	0	0	0	0	0	1	0
unknown	0	0	0	0	0	0	0	0	0	1

4.5 Results

The results are classified into three parts. The first one shows the success feature matching techniques in terms of accuracy tables, while the second part shows the runtime of each technique. Finally, a presentation on the effectiveness of the proposed approach is compared to other techniques.

4.5.1 Technique Accuracy. For each landmark, there were 100 tests performed and the successful ones divided by the total tests represent the accuracy. The accuracy is computed as the total matches divided by the total tests for each landmark.

The accuracy of the applied feature extraction techniques on our complete set of images can be classified into two ranks. The first rank is the high performance techniques for which the accuracy rate is summarized in Table 10. Beside our proposed hybrid ORB/SURF technique, two other techniques, SURF/SURF and SIFT/SIFT, showed better matching results on the modern/historic image sets. Figure 18 shows the accuracy comparison of each of the standard techniques SIFT/SIFT and SURF/SURF as well as the hybrid ORB/SURF technique.

In the matching process of modern to historic images it was found that the descriptors extracted by SURF extractor based on keypoints detected by ORB detectors are more effective than standard techniques.

This is particularly true in the sense of the number of detected points and the accurate matching of keypoints. We hypothesize that the ORB binary detectors outperform the SURF detector because the ORB detector takes advantage of its dependency on the intensity threshold parameter between the center pixel and the circular ring about the center with a measure of cornerness which is enhanced by a scale-pyramid

Table 10: Accuracy of high performance image matching techniques for each landmark, with highest accuracy rates in bold

Landmarks	SIFT/SIFT Accuracy	SURF/SURF Accuracy	ORB/SURF Accuracy
Coliseum	54%	40%	**69%**
Dome	27%	37%	**39%**
Eiffel	73%	63%	**77%**
Empire	30%	46%	**70%**
Hagia	23%	25%	**28%**
Machu	27%	33%	**40%**
Pyramid	16%	14%	**26%**
Stonehenge	28%	22%	**33%**
Taj	22%	29%	**32%**
Whitehouse	34%	33%	**46%**
Overall	33.40%	34.10%	**46.00%**

of the image. The SURF descriptors on the ORB detected features are generated through defining the subregion around the identified feature and consists of an array of 64 floating point numbers, which increases the distinctiveness within the descriptor.

The other techniques showed a poor performance on modern to historic image matching as shown in Figure19.

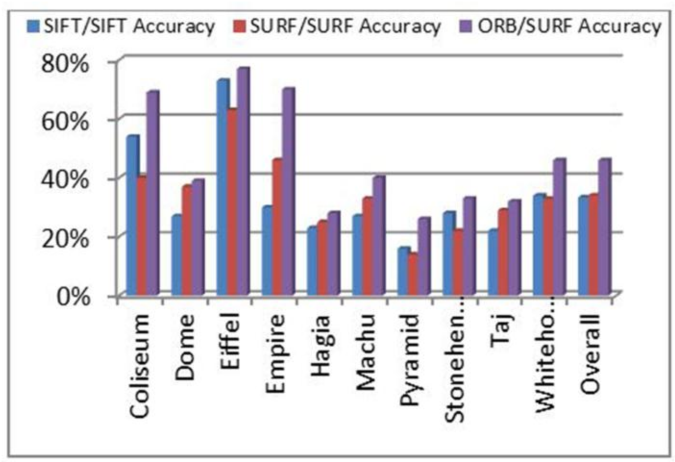

Figure 18: High performance feature matching techniques accuracy comparison

4.5.2 Runtime. The computation efforts of each technique for dealing with modern to historic images can be estimated by recording and analyzing the runtime taken by each technique on each image pair matching of all test operations. An extensive monitoring and recording of test times on an Intel Core i7-3770 3.40 GHz CPU produced the summarized runtime table (Table 11) shown below which shows the average required runtime of each of the high performance techniques on a pair of images:

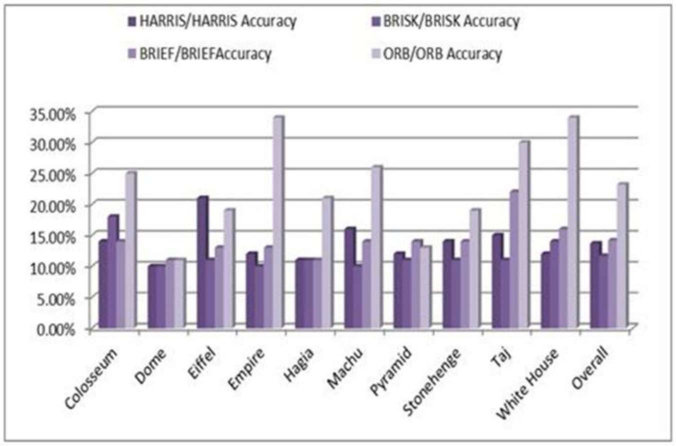

Figure 19: Low performance feature matching techniques accuracy comparison

Note in Table 11 that the SURF/SURF technique outperforms the other two techniques, followed by ORB/SURF and then SIFT/SIFT. This may not affect the overall performance of the ORB/SURF since our working environment is off-line and no critical computation is required.

Table 11:Runtime of high performance matching techniques

Techniques	SIFT/SIFT	SURF/SURF (Threshold 400)	ORB /SURF ORB(1000 points)
Runtime in ms	7.534	5.575	6.734

4.5.3 ORB/SURF Effectiveness. The evaluation of ORB/SURF technique compared to other standard and recent techniques showed that this technique outperforms other techniques in modern to historic image matching. Tables 5 and 6 shows that this technique improves the behavior of SURF/SURF and SIFT/SIFT extraction techniques and some of the tested recent techniques like BRIEF/BRIEF and BRISK/BRISK. Table 11 showed an acceptable runtime of ORB/SURF compared to other techniques.

5 Conclusion

Presentation of historic information about a geographical location or landmark represents an attractive means of sequencing historical images through a multimedia format. This may be achieved by matching modern photos to historic photos of a location or landmark.

Modern to historic photo matching represents a challenge in the sense that the historic photos have been captured by a photographer, on film, and these photos have been converted into digital format. This conversion leads to the loss of basic image characteristics in addition to the fact that these images may originally be of low quality due to paper degradation. In the matching process of modern to historic photos, a set of landmarks images was collected and classified to keep the most technically suitable ones that were all taken from a similar viewpoint. Dealing with old technology such as the pinhole camera with or without lenses alongside modern electronically captured photos with precise lenses makes the problem difficult. Available panorama making software was not designed or prepared to deal with historic photos or missing important information about camera lenses and focal length. Moreover, the problem suffers from issues such as noise, distortion and digitization artefacts in the historic photos.

The matching done using standard techniques like SIFT, SURF and ORB with vector-based or binary-based descriptors is shown to be unsuitable to resolve this problem. In an attempt to achieve an effective matching process, a novel application of the ORB/SURF was applied and this technique , although found to outperform the standard techniques, was still not sufficient for handling larger data sets, and more effort must be done searching for better techniques to deal with the problem of historic photos.

References

[1] A. Alahi, R. Ortiz, and P. Vandergheynst, "FREAK: Fast Retina Keypoint," IEEE Conference on Computer Vision and Pattern Recognition (CVPR), pp. 510-517, 2012.

[2] ArcSoft Panorama Maker - Easily Create Your Own Perfect, April 9, 2014.

[3] S. Argawal, N. Snavely, I. Simon, S. M. Seitz and R. Szeliski, "Building Rome in a Day," IEEE 12th International Conference on Computer Vision (ICCV), pp. 72-79, 2009.

[4] Autopano Giga - Home | Image-stitching software, April 9, 2014.

[5] H. Bay, T. Tuytelaars, and L. V. Gool, "Surf: Speeded up Robust Features, "*Computer Vision and Image Understanding* (*CVIU*), 110(3):346-359, 2008.

[6] M. Calonder, V. Lepetit, C. Strecha, and P. Fua, "BRIEF: Binary Robust Independent Elementary Features," *Proceedings of the 11th European Conference on Computer vision: Part IV*, pp. 778-792, 2010.

[7] J. Campbell, "Film and Cinema Spectatorship: Melodrama and Mimesis," *Polity*, 2005.

[8] http://en.wikipedia.org/wiki/Camera, April 9, 2014

[9] http://en.wikipedia.org/wiki/Dry_plate, April 9, 2014.

[10] http://en.wikipedia.org/wiki/History_of_the_camera, April 9, 2014.

[11] http://en.wikipedia.org/wiki/Photographic_film, April 9, 2014.

[12] C. M. Falco, "Ibn al-Haytham and the Origins of Computerized Image Analysis," *Proceedings of the International Conference on Computer Engineering & Systems*, ICCES '07, pp. xx - xxiii, 2007.

[13] C. Harris and M. Stephens, "A Combined Corner and Edge Detector," *Proceedings of the Alvey Vision Conference*, pp. 147-151, 1988.

[14] Y. Ke and R. Suthankar, "PCA-SIFT: A More

Distinctive Representation for Local Image Descriptors," *Proceedings of the IEEE Computer Society Conference on Computer Vision and Pattern Recognition*, 2:506-513, 2004

[15] D. G. Lowe, "Distinctive Image Features from Scale-Invariant Keypoints," *International Journal of Computer Vision*, 60(2):91-110, 2004.

[16] B. Lucas and T. Kanade, "An Iterative Image Registration Technique with an Application to Stereo Vision," *Proceedings of the 7th International Joint Conference on Artificial Intelligence*, pp. 674-679, 1981.

[17] S. Marilyn; D. Cateforis, S. Addiss, "Art History," 2nd ed, *Upper Saddle River, New Jersey: Pearson Education*, pp. 964-967, 2005.

[18] C. Michael, *The Origins of Photojournalism in America*, Smithsonian Institution Press, 1992.

[19] M. S. Nixon and A. S. Aguado, *Feature Extraction & Image Processing for Computer Vision*, 3rd Ed. Academic Press, 2012.

[20] Northlight Images, April 10, 2014.

[21 Opencv, Common Interface of Descriptor Matchers http://opencv.willowgarage.com/documentation /cpp/features2d_common_interfaces_of_descriptor _matchers.html, September 19,.2013.

[22] M. R. Peres, *The Focal Encyclopedia of Photography*, 4thed, Focal Press, 2007.

[23] PhotoStitcher photo stitching software, April 9, 2014

[24] PTGui: Photo Stitching Software 360 Degree Panorama, April 9, 2014.

[25] E. Rosten, R. Porter, and T. Drummond, "Faster and Better: A Machine Learning Approach to Corner Detection," *IEEE Transactions on Pattern Analysis and Machine Intelligence*, 32(1):105-119, January 2010.

[26] E. Rublee, V. Rabaud, K. Konolige, and G. Bradski, "ORB: An Efficient Alternative to SIFT or SURF," 2011 IEEE International Conference on Computer Vision, pp. 2564-2571, 2011.

[27] N. Snavely, R. Garg, S. M. Seitz and R. Szeliski, "Finding Paths through the World's Photos," *Proceeding SIGGRAPH ACM*, 27(3):15:1-15:11, 2008.

[28] N. Steven, M. Seitz and R. Szeliski, "Modeling the World from Internet Photo Collections," *International Journal of Computer Vision*, 80(2):189-210, 2007.

[29] http://www.societyofrobots.com/programming_ computer_vision_tutorial_pt3.shtml, April 9, 2014.

[30] H. P. Trivedi and S. A. Lioyd, "The Role of Disparity Gradient in Stereo Vision," *Perception 14*:685-690, 1985.

[31] S. Uttama, M. Coustaty, and J. M. Ogier, "Feature Extraction for Historical Image Indexing and Matching," *Proceedings of CIFED*, Bordeaux, France, pp. 247-254, 2012.

[32] A. Whitehead and J. Opp, "Timescapes: Putting History in Your Hip Pocket," *Proceedings of Computers and Their Applications Conference* (CATA, Hawaii, USA), pp. 261-266, March 2013.

Appendix A

Table A-1: Empire State Building landmark matching using HARRIS/HARRIS matcher

HARRIS/HARIS	1936	1940	1942	1955	1957	1959	1996	2007	2007b	2011
1936	1	0	0	0	0	0	0	1	0	0
1940	0	1	0	0	0	0	0	0	1	0
1942	0	0	1	0	0	0	0	0	0	0
1955	0	0	0	1	0	1	0	0	0	0
1957	0	0	0	0	1	0	0	0	0	0
1959	1	0	0	1	0	1	0	1	0	0
1996	0	0	0	0	0	0	1	0	0	0
2007	1	0	0	1	0	1	1	1	0	0
2007b	0	1	0	0	0	0	0	0	1	0
2011	0	0	0	0	0	1	0	0	0	1

Table A-2: Empire State Building landmark matching using SIFT/SIFT matcher

SIFT/SIFT	1936	1940	1942	1955	1957	1959	1996	2007	2007b	2011
1936	1	0	0	0	0	0	0	0	0	0
1940	0	1	1	0	0	1	0	0	0	0
1942	0	1	1	0	0	0	0	0	0	1
1955	1	0	0	1	0	0	0	0	0	0
1957	0	0	0	1	1	1	0	0	0	0
1959	0	1	0	0	0	1	1	0	0	1
1996	0	0	1	1	0	0	1	1	0	1
2007	0	0	0	0	0	0	1	1	0	1
2007b	0	0	0	0	0	1	0	0	1	1
2011	0	0	0	0	0	1	0	1	0	1

Table A-3: Empire State Building landmark matching using BRIEF/BRIEF matcher

BRIEF/BRIEF	1936	1940	1942	1955	1957	1959	1996	2007	2007b	2011
1936	1	0	0	0	0	0	0	0	0	0
1940	0	1	0	0	0	0	0	0	1	0
1942	0	0	1	0	0	0	0	0	0	0
1955	0	1	0	1	0	0	0	0	0	0
1957	0	0	0	0	1	0	0	0	0	0
1959	0	0	0	0	0	1	0	0	0	0
1996	0	0	0	0	0	0	1	0	0	0
2007	0	0	0	0	0	0	0	1	0	0
2007b	0	1	0	0	0	0	0	0	1	0
2011	0	0	0	0	0	0	0	0	0	1

Table A-4: Empire State Building landmark matching using BRISK/BRISK matcher

BRISK/BRISK	1936	1940	1942	1955	1957	1959	1996	2007	2007b	2011
1936	1	0	0	0	0	0	0	0	0	0
1940	0	1	0	0	0	0	0	0	0	0
1942	0	0	1	0	0	0	0	0	0	0
1955	0	0	0	1	0	0	0	0	0	0
1957	0	0	0	0	1	0	0	0	0	0
1959	0	0	0	0	0	1	0	0	0	0
1996	0	0	0	0	0	0	1	0	0	0
2007	0	0	0	0	0	0	0	1	0	0
2007b	0	0	0	0	0	0	0	0	1	0
2011	0	0	0	0	0	0	0	0	0	1

Table A-5: Empire State Building landmark matching using ORB/ORB matcher

ORB/ORB	1936	1940	1942	1955	1957	1959	1996	2007	2007b	2011
1936	1	0	0	0	0	0	0	0	0	1
1940	0	1	0	0	0	0	0	0	0	0
1942	0	0	1	0	0	0	0	0	0	0
1955	0	0	0	1	0	0	0	1	1	0
1957	1	0	1	1	1	0	0	1	0	0
1959	0	1	0	1	1	1	0	1	1	1
1996	0	0	0	0	0	1	1	1	1	1
2007	0	0	0	0	0	1	1	1	0	1
2007b	0	1	1	0	0	0	1	0	1	0
2011	0	0	0	0	0	0	0	1	0	1

Heider K Ali is doing his PhD in Electrical and Computer Engineering at Carleton University. He works on the feature matching of modern to historic photos matching of many worldwide landmarks and the investigation of the problems of dealing with historic photos. He got his MSc in computer engineering in 1991 and BSc in control and systems engineering in 1986 both from the University of Technology, Iraq. From 1993-1999 he worked in many Iraqi universities and in the period from 1999 to 2010 he worked in many universities in Jordan and Bahrain. His fields on interest are computer vision, panorama building, historic to modern photos matching, software engineering and machine learning.

Anthony Whitehead is an Associate Professor and Director of the School of Information Technology at Carleton University. He is also the current Chair of the Human Computer Interaction Program at Carleton University. His research interests can be described as practical applications of machine learning, pattern matching and computer vision as they relate to interactive applications (including games), computer graphics, vision systems and information management.